A Novel Machine Learning Based Algorithm for Efficient Streak Detection

Elisabeth Rachith[(1)], Stephan Hellmich[(1)], Belén Yu Irureta-Goyena[(1)]

[(1)]Laboratory of Astrophysics EPFL LASTRO, Observatoire de Sauverny, CH-1290 Versoix

elisabeth.rachith@epfl.ch

1 abstract

The orbit around the Earth is a busy place. After six decades of space exploration and exploitation, the safety of our assets in orbit can only be ensured by collision avoidance maneuvers by active satellites. It was further realized that active space debris removal will become necessary to ensure the usability of certain orbits.

Despite the enormous observational effort by numerous space surveillance networks, required to precisely follow the ever-growing number of space objects for conjunction prediction, very little is known about the rotational and physical properties of defunct satellites and space debris. This information is essential for active space debris removal efforts, but the disparity in requirements of the main observing objectives makes it difficult to gather. In particular, monitoring requires observations of the whole population, but only a few data points per object are needed to determine or refine its orbit; conversely, attitude determination and physical characterization focus on a subset of the population, with continuous observations of each object for the purposes of data analysis. Further, these differences are also reflected in the observational setup needed for the two tasks: on one hand, tracking is usually done with radars and ultra-wide-field telescopes that cover a large area of the accessible sky to capture as many objects as possible with a single observation; on the other hand, characterization requires dedicated observations, usually performed using mid-sized optical telescopes.

We aim to fill in this gap by extracting and analyzing observations of space objects from the VST/OmegaCam data archive. The exceptional sensitivity and photometric precision of the instrument allows us to detect targets as small as about 5 cm in LEO and 30 cm in GEO. Processing the archive, consisting of more than 400000 individual observations acquired over the past 12 years, requires highly advanced image-processing techniques. We will present our innovative streak detection method which is based on the Deep-Hough-Transform-Line-Priors algorithm developed by Lin et al. The algorithm is composed of a Lookup-based Convolutional Neural Network (LCNN) architecture, widely used in the field of shape and object recognition, with an additional layer that introduces a Hough transform in order to refine the detection of straight lines specifically. Hough-transform-based line-detection methods are already widely used for the detection of debris and satellite tracks on astronomical images and their combination with machine learning provides a better adaptability and greatly improves processing speed. To tailor the algorithm to our specific use, we built a training and validation dataset of more than 6000 hand-annotated images from the VST database. Introducing synthetic streaks to this dataset further allows us to precisely quantify the detection efficiency of the network. We present a detailed performance analysis of the algorithm in terms of achievable signal-to-noise ratio (SNR), processing speed and detection accuracy. The annotated streaks from the training and validation dataset were further used to implement and test the photometric reduction methods that are required to extract light curves from the detected streaks and to determine the rotational properties of the observed objects.

Obtaining additional data on the situation of space debris and satellites in orbit is of extreme importance given the increasing risks involved. The results of this work are very important for target selection of

future active space debris removal missions and will further help to understand the rotational evolution of defunct satellites and space debris. The precise photometric measurements will also allow us to better quantify the impact of the remaining space objects on astronomical observations, information that is important to develop mitigation strategies for future space missions, especially those involving mega-constellations with thousands of satellites.

2 Introduction

In order to carry out collision-avoidance manoeuvres as effectively as possible, to enable active debris removal missions to approach targets or, more generally, to gain a better understanding of the space environment in which we operate, it is essential to obtain and analyse data that is as accurate and complete as possible. The orbital elements of most of the largest objects are known and regularly updated, thanks to large telescope and radar networks that track space debris on a daily basis[1]. However, in addition to the lack of precision and completeness from which these catalogues sometimes suffer, particularly for high orbits [2], intrinsic characteristics, such as shape, material or rotational state, are in most cases unknown, albeit essential for the above-mentioned operations [3] [12] [14].

Our research aims to address the lack of information on the physical properties of objects and to improve the statistical knowledge of the general population of space debris by studying archival images from large telescopes primarily used for astrophysical research, using innovative debris and satellite-track detection techniques, and photometric analysis tools.

3 Data

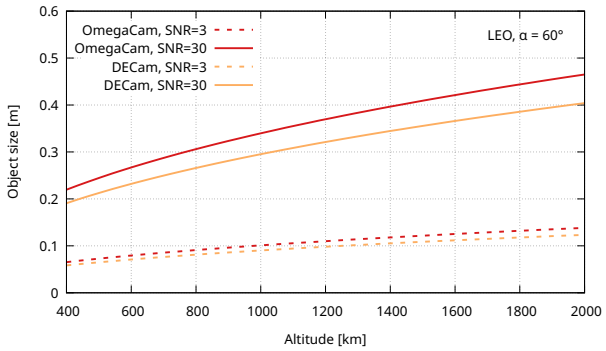
Every year, astronomical research generates thousands of images of the night sky, captured by the world's largest and most powerful telescopes. Although space debris is not the main focus of astronomical observations, both debris and active satellites in orbit inevitably pass in front of telescope sensors and, when illuminated by sunlight, leave visible traces on the images captured. Most of these images go through reduction pipelines before they are used, and unwanted streaks are removed by superimposing multiple exposures. The idea behind the present work is to use these same images, before the tracks are removed, to detect space debris and derive light curves to study first their rotational state and subsequently other physical properties, such as their sizes and shapes. The use of these images is of great interest for the study of space debris because, since the images are primarily produced for another purpose, their analysis does not require the use of dedicated observing stations. In addition, since the archives of these telescopes extend over several years, it is possible to carry out a statistical analysis over a long period of time, which is crucial for our understanding of the evolution of the debris population. Lastly, data from large telescopes have superior resolution and sensitivity compared to most dedicated space-debris observations, making it possible to detect and study faint debris.

The techniques developed will first be applied to images from the OmegaCam sensor mounted on the VST (VLT Survey Telescope) in Chile [8], before being applied to other archives from large field-of-view telescopes such as ZTF [1] and DECam [13].

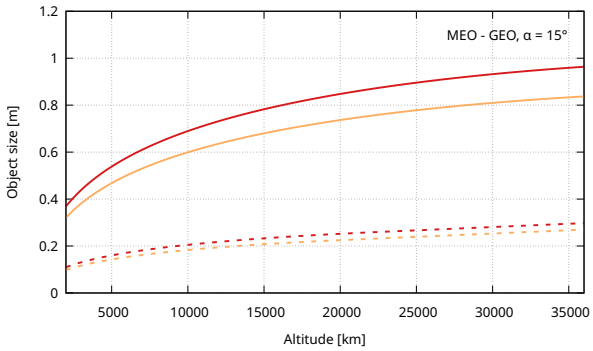
3.1 OmegaCam archive

OmegaCam is a 300-megapixel wide-field optical camera consisting of 32 individual CCDs covering one square degree with a resolution of 0.2 arcsec per pixel. The first images were taken in October 2011, and

[1] https://www.space-track.org



(a) LEO orbital regime



(b) MEO-GEO orbital regime

Figure 1: Size estimate of objects leaving a streak of SNR 3 (dashed lines) and SNR 30 (solid line) on images for different orbital regimes. From [7].

the archive comprises approximately half a million images taken over more than 10 years. Exposure times range from 30 s to 300 s. Figure 1 shows an estimate of the size of the objects we expect to see in the OmegaCam and DECam archives. We estimate streaks with SNR greater than 3 to be detectable by our algorithms and those with SNR greater than 30 to be suitable for photometric analysis. The methods used to estimate the detection limits can be found in a previous paper [7].

4 Methodology

4.1 Detection algorithm

The algorithm developed for the detection of satellite and space debris traces is a machine-learning model based on the work of Lin et al. [9], a convolutional neural network with a trainable Hough transform prior block called HT-LCNN (Hough Transform Lookup based Convolutional Neural Network). The introduction of the prior block allows for the reduction of the amount of data required during the training phase, since the model already has an initial knowledge of the shapes to look for. In fact, the Hough transform algorithm is widely used to detect lines in images.

4.2 Training, validation and test datasets

In order to tune the algorithm to our specific situation, i.e., the detection of traces in astronomical images, it is necessary to create our own dataset for training and testing the neural network. 193 VST mosaics, corresponding to 6176 individual CCD frames, were prepared for this purpose. The preparation consisted in resizing the images to remove dark edges, converting the format from FITS to PNG and applying a Zscale algorithm, since this is the preferred input format of the machine learning method, manually annotating the existing streaks by noting their start and end points, and adding artificial streaks. Artificial streaks are created by adding lines of random orientation and SNR, with widths following a Gaussian profile. The SNR is calculated locally along the streak and has values between 2 and 100. A total of 12352 artificial streaks have been added to the images, in addition to the 302 real streaks already present.

To ensure adequate validation of the algorithm, a training and validation split were created containing approximately 90% and 10% of the initial image set respectively. Data augmentation, consisting of rotation by 90 degrees, 180 degrees and 270 degrees, was applied to the training set, resulting in a total of 22328 images for training the algorithm. The validation split contains 592 images.

Finally, a test dataset containing only real streaks was created, with images that were not present in either the training or validation set, in order to assess the performance of the algorithm without the risk of bias introduced by the artificial streaks. The test dataset contains 992 images and 121 annotated streaks.

It is important to note that the data was not calibrated before the algorithm was trained or after it was used. This is to avoid downloading unnecessary data and adding extra computation time to the detection pipeline, a critical element in our research since we are dealing with extremely large amounts of data. The images in which satellite or space debris streaks are detected are calibrated for photometric analysis at a later stage.

4.3 VST analysis dataset

To perform streak analysis on a first set of unseen and unannotated data, we downloaded all the images taken by the OmegaCam in January 2022. So far, only the images taken in the r-SDSS filter have been used, representing a total of 1067 mosaics of 32 CCDs each.

4.4 Streak identification

A detailed analysis of the detected streaks requires information about the precise observing conditions, such as observer-target range, phase angle and angular velocity. In order to obtain this information, we correlated each detected streak with the catalog of known space objects maintained by the US 18th Space Defense Squadron, published on the Space Track website. Orbital information of space objects is usually provided in the form of two-line element sets (TLEs), that correspond to the mean Keplerian orbital elements at a particular epoch. The accuracy of the positions calculated from the propagation of the TLEs decreases with increasing distance from the TLE epoch. Since the VST data that we analyzed was acquired in 2022, historical TLEs are needed to identify the detected streaks with cataloged space objects. The space-track API provides access to historical orbit information, but offers only limited functionality to constrain the search. In addition, the number of queries is limited, which makes using the space-track API impractical, as we had to link thousands of streaks. Therefore, we were forced to download the entire catalog of TLEs with epochs from Jan to Feb 2022, which contained a total number of 1,480,907 individual TLEs.

For each VST image with a detected streak, we selected the TLE from each cataloged space object closest to the observation time, from an interval of 2 days around the observation time. This resulted in about 23,000 TLEs for each detection. Using the precise observation time and the astrometric solution stored along with the VST data, we were able to compute which of those objects were crossing the observed field during the exposure and projected their track into the image. This projection is of limited precision due to several reasons. First, because the TLEs that were used to compute the positions are inherently imprecise. Further, the uncertainty of positions computed by propagating the orbit, grows with increasing distance to the TLE epoch. Lastly, the astrometric solution stored along with the data is of limited precision, so even if the TLEs and propagation were perfect, the projected and detected steak would not perfectly match. To account for these uncertainties, we allowed a margin of 1000 pixels for the distance and a maximum difference of 3 degrees of the position angles between projected and detected streak. The distance margin was chosen according to an expected uncertainty in the propagated positions of about 1 km at 1000 km range and the margin for the position angle to account for a sometimes imperfect recognition of the detected streak’s slope.

4.5 Photometric reduction

One goal of our work is to determine the rotational and physical characteristics of the observed orbital debris. The information needed for this task can be extracted from photometric observations. The amount of light that is reflected from the observed object to the observer depends on the illumination geometry, the rotational phase and the object's shape and surface properties. Acquiring and examining series of brightness measurements, called light curves, makes it possible to draw conclusions about these properties even if the object is not resolved. Light curve analysis is a very powerful tool to study unresolved observations and has many applications in astronomy, ranging from characterizing Solar System objects [11] to searching for exoplanets [10] and variable stars [5]. For our analysis, we are employing the Fourier Analysis of Light Curves (FALC) algorithm [6], that applies a least-squares fit of a Fourier polynomial to the data. This technique is considered the standard method for rotation period determination of asteroids.

To obtain the light curves, we are using a similar approach to that in [3]. The intensity profile of a streak is retrieved by placing a series of rectangular apertures along the streak and measuring the flux received from the target in each aperture. We decided to use Photutils[2] to measure the fluxes, a tool that uses similar source extraction and background estimation algorithm to SExtractor and allows for user-defined aperture shapes and forced photometry on user-defined image coordinates. The time stamp of each measurement is derived from the observation time and the target's apparent angular velocity, computed from its orbital elements. The angular velocity also defines the exposure time of each measurement (the time the target spends in each measurement aperture). Knowing the exposure time allows us to obtain the apparent magnitude of the target on an absolute scale. Therefore, a set of high SNR photometric reference stars on the same field is selected from the GAIA DR2 catalog. Conversion of the magnitudes from the GAIA system to the observed band was done using the relations in [4]. Only stars with a similar color index as the Sun (V-R = 0.5 $\pm$ 0.1) were chosen. Outliers were rejected by combining the selected stars to a master reference star that was then used to compute the expected magnitude for each individual star. Reference stars with a magnitude deviation of more than 3σ from the expected value were rejected. This procedure resulted in a minimum of 15 photometric reference stars for each CCD, allowing for a robust absolute magnitude determination with an error of a few hundredths of a magnitude. From these reference stars, the magnitudes for each measurement were calculated, accounting for the corresponding exposure time, that is defined by the angular velocity of the observed object and the aperture width. Apertures contaminated by background stars or image artifacts were manually excluded.

5 Results and discussion

5.1 Precision and Recall of the detection network

The performance of the detection algorithm was assessed by analysing the results on the validation and test datasets. The absolute numbers are shown in Table 1.

The first observation that can be drawn is that the precision on the test dataset is largely inferior to the precision on the validation dataset. Recalling the formula of precision

$$P = \frac{TP}{TP + FP}, \tag{1}$$

we understand that the drop in performance is influenced by the number of false positives. However, it is interesting to note that false positives are mostly due to anomalous detections of star diffraction patterns

[2] https://photutils.readthedocs.io/en/stable/

	Validation dataset	Test dataset
Number of images	592	992
Ground truth lines (GT)	1221	121
True positives (TP)	1197	117
False negatives (FN)	24	4
False positives (FP)	67	62
Precision	95.7%	65.4%
Recall	98.0%	96.8%

Table 1: Performance of the detection algorithm on the validation and test datasets

and other linear features in the images, and if we compare the number of false positives to the total number of images analysed in both datasets, the ratio is satisfactory in the test dataset, where we have more images than in the validation dataset, and the poor performance in terms of precision can thus be explained by the ratio of ground-truth lines to the number of images.

The addition of synthetic streaks in the validation dataset artificially boosted the precision of the algorithm, but if we look at the recall of the algorithm, defined as

$$R = \frac{TP}{TP + FN} \tag{2}$$

we can see that the algorithm achieves very similar performance on both the validation and test sets. This is a good indication that the detection method remains very efficient on images containing only real space debris and satellite tracks, despite the fact that the training set contains less than 3% of real streaks.

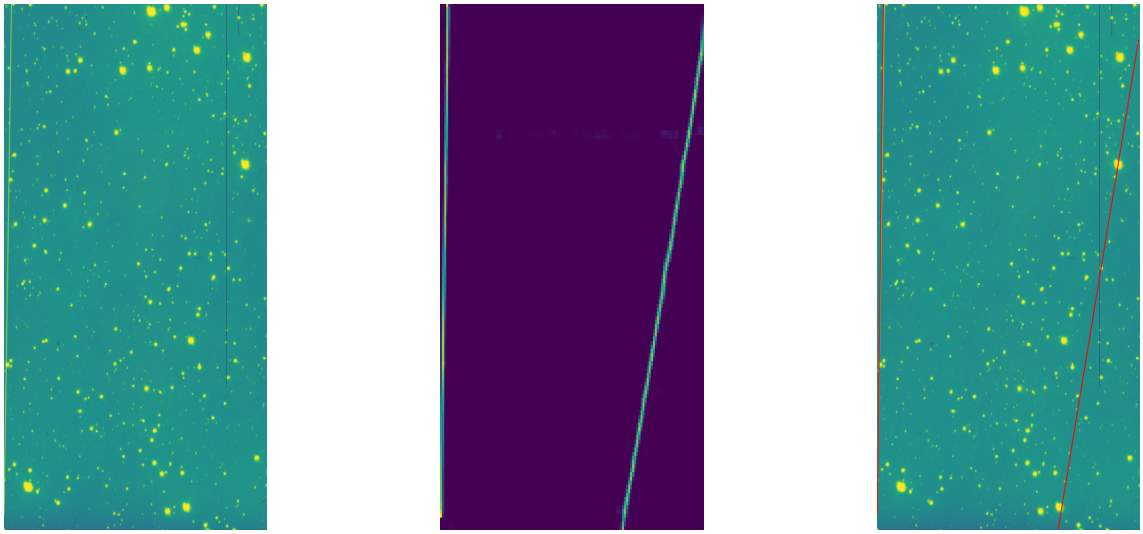
The analysis of the precision and recall metrics shows that the algorithm is very good at finding the real streaks present in the images, missing very few of them, but suffering from a high number of false positives. To partially counteract this negative effect, a detection score is used to ensure that only streaks with a detection probability above a certain threshold are considered. A threshold of 0.9 (90% probability that the detection is a space debris or satellite streak) has been chosen to ensure that most streaks are detected while reducing the number of false positives.

5.2 Achievable SNR of the detection network

The introduction of artificial streaks allows us to determine the signal-to-noise ratio limit at which the algorithm is able to detect lines. Analysis of the validation dataset shows that most streaks at SNR 3 are correctly detected, while streaks at SNR 2 are not, confirming our initial prediction of a detectability limit of SNR 3. Figure 2 shows the detection results on two streaks of SNR 46 and SNR 3 respectively.

5.3 Streak identification

Processing the VST analysis dataset with the streak detection network resulted in a total number of 3630 individual streaks of which 1182 could be identified with known objects from the space-track catalog. In total there were 214 different objects observed: 99 active payloads, 53 rocket bodies, 59 debris and 3 objects of unknown origin. The distributions of the distances and offset angles between the detected streaks and the projection of the assigned objects indicates a robust identification (see Figure 3). The



(a) Original image (b) Detection heatmap (c) Detected lines

Figure 2: Example of a true positive detection. The streak on the right of the image has SNR 3.

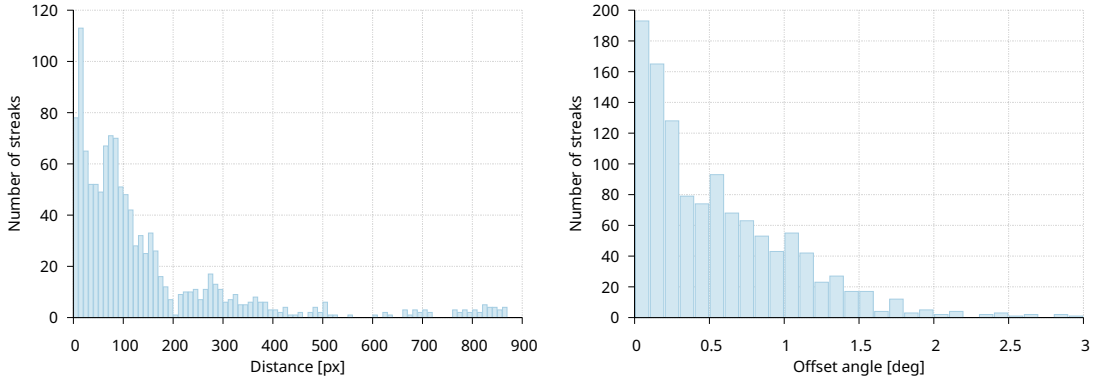


Figure 3: Distribution of the distances (left) and offset angles (right) between the detected streaks and the projection of the identified objects.

majority of correlated streaks are within 200 px and 1.5 deg of the projection of the TLE of the assigned object.

5.4 Photometric reduction

Since there are a few objects that have been detected multiple times, we were curious if it is possible to combine the individual observations. As a test, we reduced all observations of 26880 (2001-033A), a geostationary satellite that belongs to the US Air Force Defense Support Program. This object was observed by VST during 8 nights from January 2 to January 21 2022 and caused a total number of 48 streaks on 12 OmegaCam exposures. The light curves of the streaks were extracted and period fits were performed with the FALC algorithm. Figure 4 shows the results of all period fits. We identified a constant rotation rate of 9.9s, which is consistent with what is known about this object [3]. The object was observed at phase angles ranging from 6 to 18 degrees. In order to reconstruct the targets phase curve, we

[3] https://space.skyrocket.de/doc_sdat/dsp-3.htm

converted the mean magnitude of each light curve from the period fits to the reduced magnitude. Figure 5 shows the reduced magnitudes over the phase angle. While there seems to be a correlation between phase angle and reduced magnitude, fitting the data to a phase function as described in [15] did not produce a reliable phase curve.

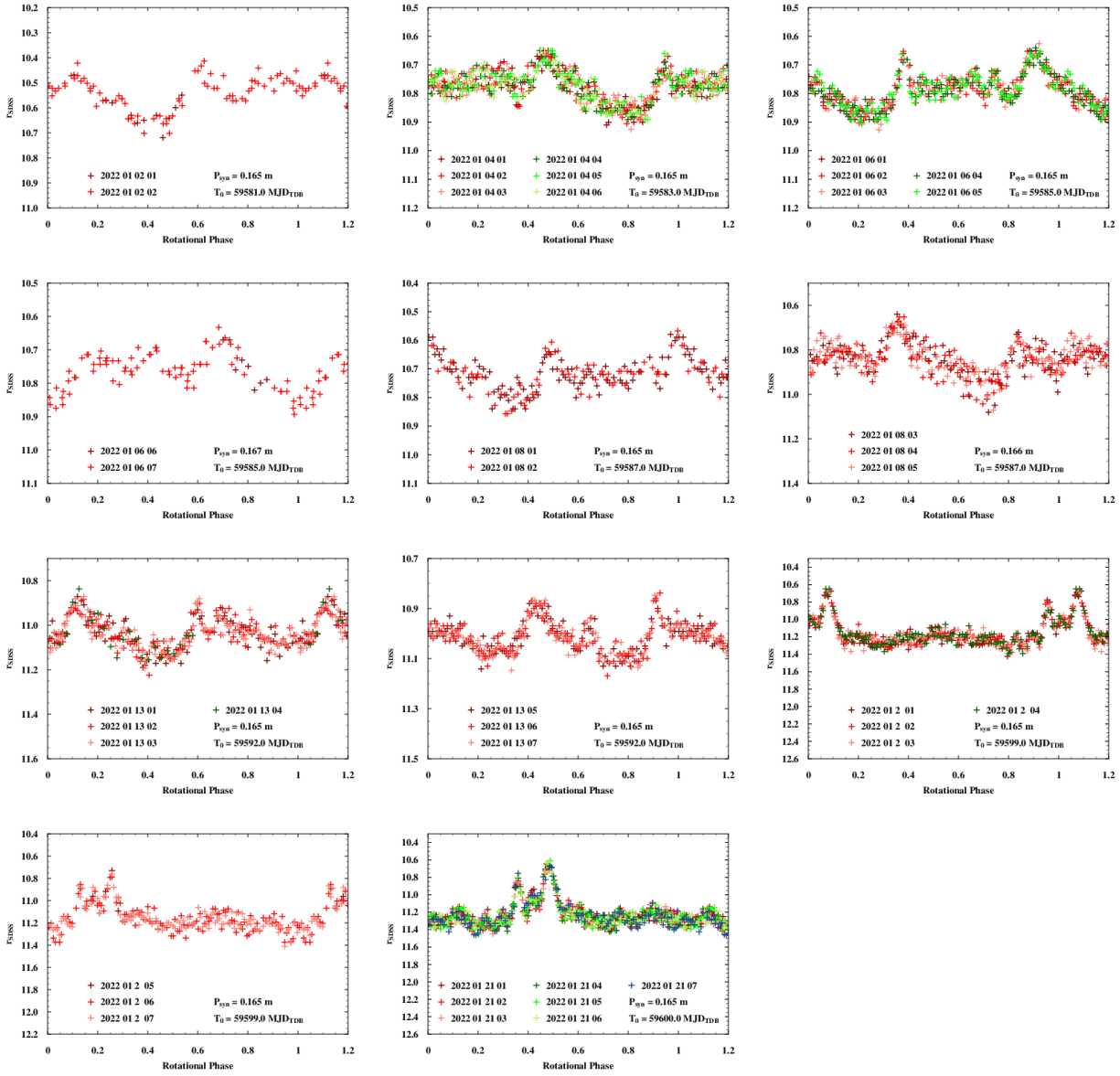


Figure 4: Period fits of all light curves measured from 26880 (2001-033A).

6 Conclusion

Our machine learning algorithm for streak detection is a significant advancement in space debris analysis. Evaluation on validation and test datasets demonstrates its effectiveness in identifying space debris and satellite streaks in astronomical images.

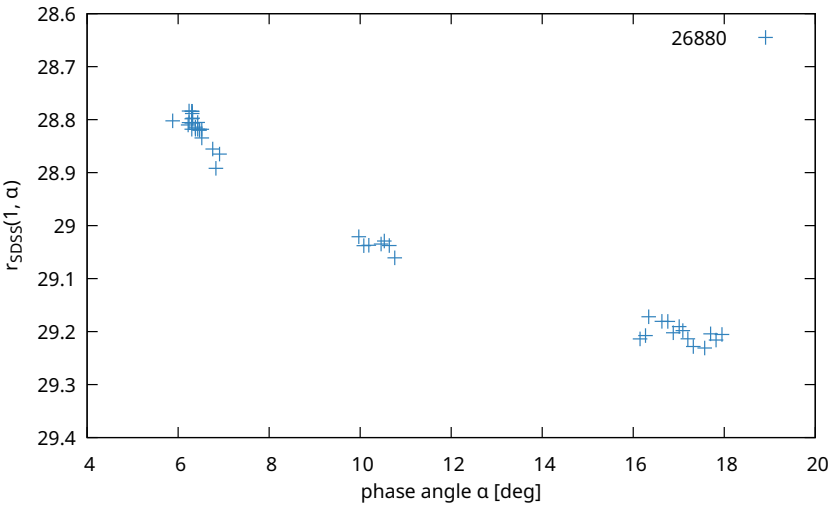


Figure 5: Reduced magnitudes over phase angle.

Applying the algorithm to the VST/OmegaCam data archive shows promising results in streak identification with known space objects. The precision in correlating detected streaks with cataloged objects, including distance and offset angles, highlights the robustness of our identification process.

The implementation of photometric reduction methods, exemplified by the analysis of geostationary satellite 26880 (2001-033A), indicates the potential for extracting rotational and physical characteristics from observed objects. The consistent rotation rate identified aligns with existing knowledge, reinforcing the reliability of our approach.

As we explore large telescope data archives, like VST, the insights from our algorithm significantly contribute to space situational awareness. Information extracted from detected streaks aids in active debris removal and helps develop mitigation strategies for future space missions. Our work opens avenues for a comprehensive understanding of the rotational evolution and physical properties of space debris, crucial for ensuring the safety and sustainability of Earth's orbital environment.

References

[1] E. C. Bellm and al. The Zwicky Transient Facility: System overview, performance, and first results. Publications of the Astronomical Society of the Pacific, 131, 2019.

[2] J. A. Blake, P. Chote, D. Pollacco, W. Feline, G. Privett, A. Ash, S. Eves, A Greenwood, N. Harwood, T. R. Marsh, D. Veras, and C. Watson. Debriswatch 1: A survey of faint geosynchronous debris. Advances in Space Research, 67(1):360–370, 2021.

[3] P. Chote, J. Blake, and D. Pollacco. Precision Optical Light Curves of LEO and GEO Objects. In Advanced Maui Optical and Space Surveillance Technologies Conference, page 52, 2019.

[4] D. W. Evans, M. Riello, F. De Angeli, J. M. Carrasco, P. Montegriffo, C. Fabricius, C. Jordi, L. Palaversa, C. Diener, G. Busso, M. Weiler, C. Cacciari, and F. van Leeuwen. Gaia Data Release 2. The photometric content and validation. Astronomy & Astrophysics, 2018.

[5] L. Eyer and N. Mowlavi. Variable stars across the observational HR diagram. Journal of Physics: Conference Series, 118, 2008.

[6] A.W. Harris, J.W. Young, E. Bowell, L.J. Martin, R.L. Millis, M. Poutanen, F. Scaltriti, V. Zappalà, H.J. Schober, H. Debehogne, and K.W. Zeigler. Photoelectric observations of asteroids 3, 24, 60, 261, and 863. Icarus, 77:171–186, 1989.

[7] S. Hellmich, E. Rachith, B. Y. Irureta-Goyena, and J.-P. Kneib. Harvesting large astronomical data archives for space debris observations. In 2nd NEO and Debris Detection Conference, volume 2. ESA Space Debris Office, 2023.

[8] K. Kuijken. OmegaCAM: ESO's newest imager. The Messenger, 146:8, 2011.

[9] Y Lin, S. L. Pintea, and J. C. van Gemert. Deep hough-transform line priors. In Computer Vision – ECCV 2020, pages 323–340. Springer International Publishing, 2020.

[10] J. Miralda-Escudé. Orbital Perturbations of Transiting Planets: A Possible Method to Measure Stellar Quadrupoles and to Detect Earth-Mass Planets. The Astrophysical Journal, 564(2), 2002.

[11] P. Scheirich, P. Pravec, S.A. Jacobson, J. Ďurech, P. Kušnirák, K. Hornoch, S. Mottola, M. Mommert, S. Hellmich, D. Pray, D. Polishook, Yu.N. Krugly, R.Ya. Inasaridze, O.I. Kvaratskhelia, V. Ayvazian, I. Slyusarev, J. Pittichová, E. Jehin, J. Manfroid, M. Gillon, A. Galád, J. Pollock, J. Licandro, V. Alí-Lagoa, J. Brinsfield, and I.E. Molotov. The binary near-Earth Asteroid (175706) 1996 FG3 — An observational constraint on its orbital evolution. Icarus, 245:56–63, 2015.

[12] T. Schildknecht, T. Flohrer, and A. Vananti. ESA optical surveys to characterize recent fragmentation events in GEO and HEO. In 1st NEO and Debris Detection Conference, volume 1. ESA Space Debris Office, 2019.

[13] E. Sánchez. The Dark Energy Survey. Journal of Physics: Conference Series, 259, 2010.

[14] J. Šilha, S. Krajčovič, M. Zigo, J. Tóth, D. Žilková, P. Zigo, L. Kornoš, J. Šimon, T. Schildknecht, E. Cordelli, A. Vananti, H. K. Mann, A. Rachman, C. Paccolat, and T. Flohrer. Space debris observations with the slovak AGO70 telescope: Astrometry and light curves. Advances in Space Research, 65(8):2018–2035, 2020.

[15] J. Šilha, M. Zigo, T. Hrobár, P. Jevčák, and M. Verešvárska. Light curves application to space debris characterization and classification. 8th European Conference on Space Debris, 2021.